DALTON
FULL PAPER

# Dichloro(1,4,8,11-tetraazacyclotetradecane)manganese(III) chloride: *cis–trans* isomerisation evidenced by infrared and electrochemical studies

**Fabien Létumier,[a] Grégory Broeker,[a] Jean-Michel Barbe,[a] Roger Guilard,*,†,[a] Dominique Lucas,[b] Valérie Dahaoui-Gindrey,[c] Claude Lecomte,*,[c] Laurent Thouin[d] and Christian Amatore*,[d]**

[a] *Laboratoire d'Ingénierie Moléculaire pour la Séparation et les Applications des Gaz (LIMSAG, UMR 5633), Faculté des Sciences 'Gabriel', 6, Bd Gabriel, 21100 Dijon, France*
[b] *Laboratoire de Synthèse et d'Electrosynthèse Organométallique (LSEO, UMR 5632), Faculté des Sciences 'Gabriel', 6, Bd Gabriel, 21100 Dijon, France*
[c] *Laboratoire de Cristallographie et Modélisation des Matériaux Minéraux et Biologiques (LCM3B), UPRESA 7036, Université Henri Poincaré, Nancy 1, Faculté des Sciences, B.P. 239, 54506 Vandoeuvre lès Nancy Cedex, France*
[d] *Ecole Normale Supérieure, Département de Chimie, URA CNRS 1679, 24, rue Lhomond, 75231 Paris, Cedex 05, France*



The isomers *cis*- and *trans*-dichloro(1,4,8,11-tetraazacyclotetradecane)manganese(III) chloride have been synthesized and characterised. An isomerisation of the type *cis*-$Mn^{III}$ ⟶ *trans*-$Mn^{III}$ was observed by IR spectroscopy. Recrystallisation of the *cis* species gave systematically crystals of the *trans* derivative. The crystal structure of the latter complex has been determined. An electrochemical study of the *trans*-manganese(III) complex in dimethyl sulfoxide revealed a rare *trans* ⟶ *cis* isomerisation reaction which proceeds through an electrochemical step–chemical step mechanism. The overall first-order rate constant, $k_{iso}$, for this isomerisation was determined by simulation of the chronoamperometric data. Supplementary electrochemical information for the *trans*-manganese(III) isomer was obtained through simulation of the cyclic voltammograms over a large range of scan rates. No influence of chloride ion concentration was observed as determined by cyclic voltammetry using an internal chloride standard, $[N(PPh_3)_2]Cl$. The cyclic voltammogram of the *cis*-dichloro(1,4,8,11-tetraazacyclotetradecane)manganese(II) generated *in situ* displays the usual *cis* ⟶ *trans* isomerisation which also occurs *via* an electrochemical step–chemical step mechanism.

Manganese is involved in many biological processes, in particular it is the active site of several enzymes.[1–3] In order to mimic these enzymes, many manganese polyazamacrocyclic complexes have been synthesized and studied in connection with oxidation state,[4] co-ordination scheme[5] and number of manganese sites present in these biological catalysts.[6,7] As an example, manganese pentaazamacrocyclic complexes have been prepared and characterised in efforts to determine the mechanism of action of superoxide dismutase.[8] Furthermore, parallel syntheses of porphyrin and triazamacrocycle manganese complexes have been carried out and these complexes have been shown to be catalytically active in oxidation reactions.[9–14] In these latter derivatives the oxidation state of the metal centre is II, III, or IV, their structure varying from monomer up to tetramer.[15–17] Two types of manganese cyclam complexes have been found to be important in catalytic oxidation reactions: a mixed-valence dinuclear complex of the type $Mn^{III}$–$Mn^{IV}$ [18–20] and a *trans*-dichlorocyclam manganese(III) species.[21] However, the active form of the 1,4,8,11-tetraazacyclotetradecane (cyclam) manganese complex involved in these oxidation reactions remains unknown.[22,23] In the present work, we have synthesized and characterised a third type of cyclam manganese complex, the *cis*-dichlorocyclam manganese(III) chloride. In addition, a *cis* ⟶ *trans* isomerisation reaction has been observed and monitored by IR spectroscopy. Complementary information has been provided through electrochemical studies where both *cis* ⟶ *trans* [24,25] and, a more rarely observed, *trans* ⟶ *cis* isomerisation reactions [26,27] occur as the precursors are oxidised or reduced respectively. Efforts have been made to crystallise the *cis* complex, but systematically crystals of the *trans* isomer have been produced *via* the above mentioned *cis* ⟶ *trans* isomerisation reaction. The crystal structure of this latter derivative is reported.

† E-mail: rguilard@u-bourgogne.fr

## Experimental

### Instrumentation

Cyclic voltammetry experiments were performed using a model 273A EG&G potentiostat controlled by a personal computer using the EG&G 270/250 Research Electrochemistry Software (version 4.23). These experiments were carried out in a three-electrode cell using a glassy carbon disc ($r = 1.5$ mm) as the working electrode, a platinum spiral as the counter electrode, and a saturated calomel electrode (SCE) as the reference. In experiments at higher scan rate the working electrode was a platinum disc ($r = 0.025$ mm). The cyclic voltammetry was simulated using the DIGISIM program (version 2.1) distributed by the Bioanalytical Systems Corporation.[28] For the coulometric measurements a IG6-N Tacussel instrument was used. The potentials were held constant with a model 362 EG&G potentiostat. In the electrolyses a carbon tissue was used as the working electrode, and the counter electrode was either a platinum spiral or magnesium ribbon. The counter electrode compartment was separated from the working electrode with a porous glass sintered disc. Experiments using a rotating disc electrode (RDE) were accomplished with a gold electrode ($r = 1$ mm, Tacussel). Rotation speeds of 900 revolutions $min^{-1}$ yielded stationary-state voltammograms. Double-step chronoamperometry was performed using the same electrodes as in the experiments at the elevated scan rates. Three different concen-

trations were analysed: 0.5, 1.0 and 2.0 mM over time intervals of 5 to 200 ms. The programmed potential ramp began and ended approximately 200 mV before and after the peak of the corresponding reduction wave in the cyclic voltammetry for the equivalent time interval. All potentials are referred to the SCE; electrochemical experiments were conducted at room temperature.

The IR spectra were recorded on a Bruker IFS 66v FTIR spectrometer and samples were prepared as 1% dispersions in KBr pellets.

### Chemicals

The cyclam ligand was prepared in our laboratory following literature methods.[29,30] For all syntheses, chemicals were commercially available and used as received without further purification. For the electrochemical studies, dimethyl sulfoxide (dmso) was dried over activated 3 Å molecular sieves. Bis(triphenylphosphoranylidene)ammonium chloride $[N(PPh_3)_2]Cl$ was from Aldrich. The electrolyte support, tetra-*n*-butylammonium hexafluorophosphate (Fluka), was used as received.

**Di-μ-oxo-bis(1,4,8,11-tetraazacyclotetradecane)dimanganese(III,IV) perchlorate.** This compound is formed during the preparation of the *cis*-$[Mn(cyclam)Cl_2]Cl$ (see below). It was synthesized using a slightly different procedure than that described.[19,20] A solution of $Mn(ClO_4)_2\cdot 6H_2O$ (1.8 g, 5 mmol) in methanol (50 $cm^3$) and water (10 $cm^3$) was added dropwise to cyclam (1 g, 5 mmol) in methanol (20 $cm^3$). The resultant mixture turned olive green. After stirring for 1 h, it was filtered and a green precipitate recovered after several washings with cold methanol. The precipitate was then air-dried. **CAUTION**: care should be taken in isolation of the solid product; transition metal perchlorates are potentially explosive and must be prepared in small amounts. Yield 1.43 g (33%) (Found: C, 27.7; H, 5.8; N, 12.9. Calc. for $C_{20}H_{48}Cl_3Mn_2N_8O_{14}\cdot H_2O$: C, 27.9; H, 5.8; N, 13.0%).

***trans*-Dichloro(1,4,8,11-tetraazacyclotetradecane)manganese(III) chloride.** A solution of $Mn(CH_3CO_2)_3\cdot 2H_2O$ (6.7 g, 25 mmol) in methanol (200 $cm^3$) was added to cyclam (5 g, 25 mmol) dissolved in methanol (50 $cm^3$). The reaction mixture was then stirred for 3 h at room temperature. Concentrated HCl (1 $cm^3$) was then added to allow the formation of a clear green precipitate which was filtered off and recrystallised from water (7.33 g, 65%) (Found: C, 26.8; H, 7.6; N, 12.3. Calc. for $C_{10}H_{24}Cl_3MnN_4\cdot 5H_2O$: C, 26.6; H, 7.6; N, 12.4%).

***trans*- and *cis*-Dichloro(1,4,8,11-tetraazacyclotetradecane)manganese(III) chloride (one-pot synthesis).** A solution of $MnCl_2\cdot 4H_2O$ (1.98 g, 10 mmol) in methanol (100 $cm^3$) was added to a solution of cyclam (2 g, 10 mmol) in methanol (25 $cm^3$). The resultant solution was olive green. After evaporation of three-fourths of the solvent, a clear green precipitate was collected and, after filtration, identified as the *trans*-manganese(III) complex previously described (see above). Treatment of the filtrate [containing the mixed-valence μ-oxo-dimanganese(III, IV) species] by concentrated HCl (0.4 $cm^3$, 1 equivalent) led to the formation of a red precipitate. After filtration and washing several times with methanol, the *cis*-dichloro(1,4,8,11-tetraazacyclotetradecane)manganese(III) chloride was obtained. (1.3 g, 35%) (Found: C, 33.0; H, 6.7; N, 14.9. Calc. for $C_{10}H_{24}Cl_3MnN_4\cdot 0.33CH_3OH$: C, 33.3; H, 6.8; N, 15.0%).

### Crystallography

**Crystal data for *trans*-$[Mn(cyclam)Cl_2]Cl\cdot 5H_2O$.** $C_{10}H_{24}Cl_3MnN_4\cdot 5H_2O$, $M = 451.7$, monoclinic, space group $P2_1/n$, $a = 9.876(1)$, $b = 6.501(1)$, $c = 16.651(2)$ Å, $\beta = 107.39(1)°$, $U = 1020.3(2)$ $Å^3$, room temperature, $Z = 2$, $\mu$(Mo-K$\alpha$) = 1.09 $mm^{-1}$, 4421 reflections measured {including substructure, see below, $[\sin\theta/\lambda]_{max} = 0.6$ $Å^{-1}$}, 2105 structure reflections of which 1479 [$I \geqslant 3\sigma(I)$, $R_{int} = 0.005$] were used for the refinement. Final $R(F) = 0.036$ and $R'(F) = 0.042$.

A first quick and short data collection had shown that this manganese(III) complex crystallises in the monoclinic system with lattice type C (systematic absences: $hkl$, $h + k \neq 2n$). A total of 4421 reflections was collected. During the data treatment it became evident that reflections with $k$ odd (or $h$ odd) were much weaker than those with $k$ even (or $h$ even), and furthermore that the reflections with $k$ odd may not be averaged according to $2/m$ symmetry, indicating the existence of a substructure of lower symmetry. Then, in order to find the average structure, we only used the reflections with $k$ (or $h$) even, the new unit cell being four times smaller than the old one. This transformation led to systematic absences ($h0l$, $h + l \neq 2n$); thus this manganese complex crystallises in the monoclinic system, space group $P2_1/n$. Lorentz-polarisation corrections, intensity scaling (2% decay), and data reduction were carried out using the DREAR package.[31] No absorption correction was applied. The structure was solved by Patterson methods and successive Fourier synthesis, then refined by full-matrix least squares.[32] After location of all non-H atoms, difference electron density maps revealed three residual peaks of approximately the same weight in the asymmetric unit. Two have been attributed to oxygen atoms of water solvate molecules [w(1) and w(2)]. The third peak corresponds to a site occupied by a chloride ion [Cl(2)] and by an oxygen atom of a water molecule [w(3)], each with an occupancy factor of 50%. The positions of the Cl(2) and w(3) atoms have been alternatively refined. The two atoms are separated by 0.552(6) Å. This disorder refined in the $P2_1/n$ space group explains the weak substructure reflections due to the solvent and counter-ion structure. All attempts to solve the substructure failed. The refined parameters included anisotropic mean-square displacements for the non-H atoms, and positions for the macrocycle H atoms, isotropic mean-square displacements being $B(H) = 1.3\ B(X)$, where $B(X)$ is the equivalent isotropic mean-square displacement for atom X to which the H atom is covalently bound. The ORTEP[33] program was used to draw the crystal structure views (Figs. 1 and 2). Selected bond distances and angles are reported in Table 1, and the geometry of the intra- and inter-molecular hydrogen bonds in Table 2.

CCDC reference number 186/990.

## Results and Discussion

### Synthesis

The complexes were obtained starting from stoichiometric amounts of cyclam and manganese dichloride. Under these experimental conditions, the mixed-valence dinuclear complex $Mn^{III}$–$Mn^{IV}$ and the *trans*-dichlorocyclam manganese(III) complex are formed simultaneously at room temperature. We observed that hydrolysis of the mixed-valence dinuclear complex, in methanol, by addition of concentrated HCl led to the formation of *cis*-$[Mn(cyclam)Cl_2]Cl$ (see below). The reaction is visibly apparent, as the initial solution of $Mn^{III}$–$Mn^{IV}$ is olive green, and upon addition of HCl the solution gradually becomes red. Interestingly, the reaction with HCl seems to break the μ-oxo bridges but maintains the *cis* arrangement. In aqueous medium the *cis* isomer rapidly and irreversibly converts into the *trans* species at room temperature as has been previously observed for cobalt(III) complexes.[34,35] However, the present reaction is different from that reported for corresponding iron(III) complexes where the *cis* ⟶ *trans* conversion requires heating.[36]

### Crystal structure of *trans*-dichloro(1,4,8,11-tetraazacyclotetradecane)manganese(III) chloride

An ORTEP view of the crystal structure of the *trans*-

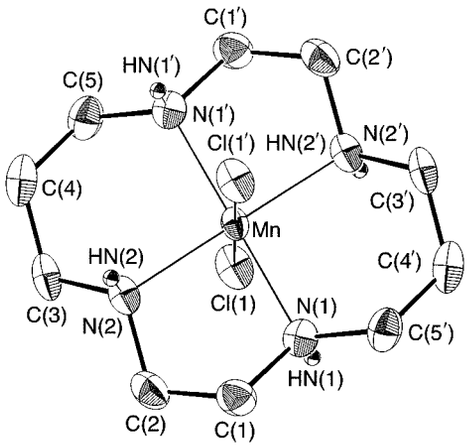


**Fig. 1** An ORTEP view of the molecular structure of the *trans*-[Mn(cyclam)$Cl_2$]Cl complex with 50% probability thermal ellipsoids for non-H atoms. Only hydrogen atoms bonded to the nitrogen atoms are shown. Atoms obtained by inversion [0, 0, 0] have primed labels

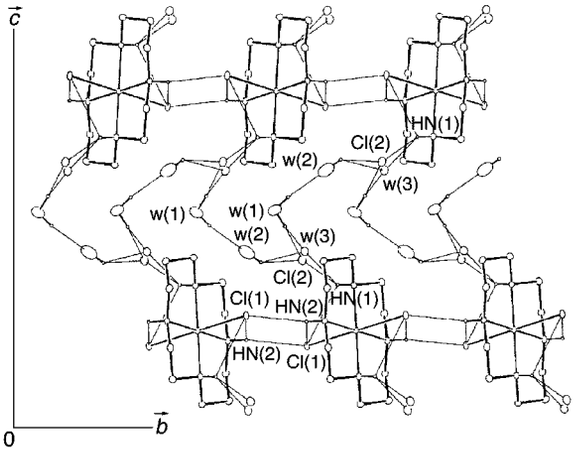


**Fig. 2** An ORTEP view of the crystal packing in *trans*-[Mn(cyclam)$Cl_2$]Cl·5$H_2O$ as a projection in the ($\vec{b}$, $\vec{c}$) plane, with 25% probability thermal ellipsoids for non-H atoms. Hydrogen bonds are indicated by single thin lines

**Table 1** Selected bond distances (Å) and angles (°) with estimated standard deviations (e.s.d.s) in parentheses for *trans*-[Mn(cyclam)$Cl_2$]Cl·5$H_2O$

| | | | |
|---|---|---|---|
| Mn–N(1) | 2.036(3) | Mn–Cl(1) | 2.5269(7) |
| Mn–N(2) | 2.031(2) | | |
| N(1)–Mn–N(2) | 85.5(1) | N(1)–Mn–Cl($1^I$) | 91.26(7) |
| N(1)–Mn–Cl(1) | 88.74(7) | N(2)–Mn–Cl($1^I$) | 91.74(7) |
| N(2)–Mn–Cl(1) | 88.26(7) | Cl(1)–Mn–Cl($1^I$) | 180 |
| N(1)–Mn–N($2^I$) | 94.5(1) | | |

Symmetry code: I $-x$, $-y$, $-z$.

[Mn(cyclam)$Cl_2$]$^+$ complex is given in Fig. 1 with the numbering scheme used. The manganese ion lies on one $\bar{1}$ inversion centre. The structure consists of centrosymmetric [Mn(cyclam)$Cl_2$]$^+$ cations which are linked by hydrogen bonds to the chloride anions and to the water molecules. The geometry at manganese is *trans*-pseudo-octahedral with the four nitrogen atoms of the ligand in equatorial position [average Mn–N 2.033(3) Å], and the two chloride ions in axial positions with a very long Mn–Cl bond length [2.5269(7) Å]. This bond distance is much longer than that found in the similar complex *trans*-[Co(cyclam)$Cl_2$]Cl·4$H_2O$·0.47HCl[37] where the distance Co–Cl is equal to 2.2524(6) Å. The Mn–N and Mn–Cl bond lengths are very similar to those of the *trans*-[Mn(cyclam)$Cl_2$]$NO_3$ complex,[21] as are the *cis* N–Mn–N bond angles of 85.5(1) and 94.5(1)°, the smaller value being associated with the five-membered ring [Mn, N(1), C(1), C(2), N(2)] as expected. In the same way, the bond distances and angles in the cyclam ligand are thoroughly consistent with those found in the literature.[21,37–39] The metal ion is located in the plane of the four nitrogen atoms. Hydrogen atoms bonded to N(1′) and N(2) are above the four-nitrogen plane, whereas the hydrogen atoms bonded to N(1) and N(2′) are below, giving rise to the expected *trans*-III conformation according to the nomenclature of Bosnich *et al.*[40] Based on the N–H bond direction relative to the four-nitrogen atom plane, five energetically distinct non-enantiomeric *cis* and *trans* isomers, denoted I to V, are conceptually possible since each co-ordinated nitrogen atoms is chiral. In the *trans*-III isomer the five-membered chelate rings adopt twist conformations, and the six-membered chelate rings are in chair conformations. Fig. 2 shows the crystal packing of *trans*-[Mn(cyclam)$Cl_2$]Cl·5$H_2O$ as a projection in the ($\vec{b}$, $\vec{c}$) plane, and the geometry of the intra- and inter-molecular hydrogen bonds is given in Table 2. The HN(2) hydrogen atom participates in a three-centre hydrogen bond,[41] involving the N2–HN(2) bond and two hydrogen bonds with the Cl(1) chloride ion as acceptor, one being an intramolecular bond and the other an intermolecular bond. That three-centre hydrogen bond gives rise to infinite chains of the [Mn(cyclam)] complex which extend along the $\vec{b}$ axis direction. The sum of the angles involving HN(2) as central atom is exactly 360°. A Mn–N(2)–NH(2)···Cl(1)–Mn interaction has also been found in the *trans*-[Mn(cyclam)$Cl_2$]$NO_3$ complex,[21] which also crystallises in the space group $P2_1/n$, but in that case the chain structure runs parallel to the $\vec{a}$ axis, the Mn···Mn separation (*i.e.* the $\vec{a}$ axis length) being 6.547(2) Å compared to 6.501(1) Å for the $\vec{b}$ axis length in our case. These infinite chains are linked to one another *via* the Cl(2) chloride ion and the water molecules. The HN(1) hydrogen atom is also involved in a three-centre hydrogen bond, on the one hand from an intramolecular contact with the Cl(1) chloride ion and on the other from an intermolecular contact with the Cl(2) ion and the w(3) water molecule. The sum of the characteristic angles of the three-centre hydrogen bond is 360 and 357°, for w(3) and Cl(2) as acceptor respectively. The intermolecular contact of 2.875(7) Å between w(1) and w(3) seems to correspond to an hydrogen bond where w(3) would be the donor.

### Characterisation of the isomerisation reaction by IR spectroscopy

The *cis*-$Mn^{III}$ ⟶ *trans*-$Mn^{III}$ isomerisation reaction can be monitored by IR spectroscopy in the region 800–900 $cm^{-1}$ where the N–H and $CH_2$ vibrations of the cyclam moiety are sensitive to the geometric nature of the ligand co-ordinated to the metal. The *cis* complexes have a distinct fingerprint pattern which is practically insensitive to the nature of the metal. Previously reported *cis* complexes of the type $M^{III}$(cyclam)$Cl_2$ exhibit two $CH_2$ (794–824 $cm^{-1}$) and three to four N–H absorption bands (841–926 $cm^{-1}$) (see Table 3).[35,36] In agreement with those studies, the *cis*-[Mn(cyclam)$Cl_2$]Cl complex presents also two bands in the region 790–830 $cm^{-1}$ and two broad and intense bands in the region 840–890 $cm^{-1}$. Another band of weaker intensity is noted at 923 $cm^{-1}$.

In a short period of time the *cis* isomer dispersed in a KBr pellet transformed into the *trans* complex. We attribute this isomerisation to trace amounts of water contained in the KBr salt. This isomerisation reaction is demonstrated through IR spectroscopy by the disappearance of the four bands at 923, 858, 844 and 807 $cm^{-1}$ and the concomitant appearance of one intense band at 880 $cm^{-1}$. Conversely, the band at 795 $cm^{-1}$ is unaffected. These two remaining bands are characteristic of the *trans* isomer (see Table 3). The evolution of the IR spectrum during the *cis* ⟶ *trans* isomerisation reaction is depicted in

**Table 2** Geometry of the intra- and inter-molecular hydrogen bonds (distances in Å, angles in °) in the *trans*-[Mn(cyclam)$Cl_2$]Cl·5$H_2O$ complex

| | | | | | | | |
|---|---|---|---|---|---|---|---|
| Intramolecular hydrogen bonds | | | | | | | |
| $Cl(1^{I})\cdots N(2)$ | 3.193(2) | N(2)–HN(2) | 0.86(4) | $HN(2)\cdots Cl(1^{I})$ | 2.72(3) | $N(2)–HN(2)\cdots Cl(1^{I})$ | 116(3) |
| $Cl(1)\cdots N(1)$ | 3.210(3) | N(1)–HN(1) | 0.76(4) | $HN(1)\cdots Cl(1)$ | 2.83(4) | $N(1)–HN(1)\cdots Cl(1)$ | 114(3) |
| Intermolecular hydrogen bonds | | | | | | | |
| $w(1)\cdots w(2)$ | 2.783(6) | w(1)–Hw(12) | 0.780(4) | $Hw(12)\cdots w(2)$ | 2.015(5) | $w(1)–Hw(12)\cdots w(2)$ | 168.4(4) |
| $w(1)\cdots w(3^{II})$ | 2.773(6) | w(1)–Hw(11) | 1.058(4) | $Hw(11)\cdots w(3^{II})$ | 1.717(5) | $w(1)–Hw(11)\cdots w(3^{II})$ | 175.1(3) |
| $w(1)\cdots Cl(2^{II})$ | 3.231(4) | | | $Hw(11)\cdots Cl(2^{II})$ | 2.174(2) | $w(1)–Hw(11)\cdots Cl(2^{II})$ | 175.7(2) |
| $w(1)\cdots w(3)$ | 2.875(7) | | | | | | |
| $w(1)\cdots Cl(2)$ | 3.024(5) | | | | | | |
| $w(2)\cdots Cl(2^{III})$ | 2.859(5) | w(2)–Hw(21) | 0.764(5) | $Hw(21)\cdots Cl(2^{III})$ | 2.240(2) | $w(2)–Hw(21)\cdots Cl(2^{III})$ | 138.8(3) |
| $w(2)\cdots w(3^{III})$ | 3.174(6) | | | $Hw(21)\cdots w(3^{III})$ | 2.632(5) | $w(2)–Hw(21)\cdots w(3^{III})$ | 129.6(3) |
| $N(1)\cdots w(3^{I})$ | 3.050(6) | N(1)–HN(1) | 0.76(4) | $HN(1)\cdots w(3^{I})$ | 2.41(4) | $N(1)–HN(1)\cdots w(3^{I})$ | 143(4) |
| $N(1)\cdots Cl(2^{I})$ | 3.238(3) | | | $HN(1)\cdots Cl(2^{I})$ | 2.56(4) | $N(1)–HN(1)\cdots Cl(2^{I})$ | 150(4) |
| $N(2)\cdots Cl(1^{IV})$ | 3.233(3) | N2–HN(2) | 0.86(4) | $HN(2)\cdots Cl(1^{IV})$ | 2.49(4) | $N(2)–HN(2)\cdots Cl(1^{IV})$ | 146(3) |

Symmetry codes: I $-x, -y, -z$; II $0.5-x, -0.5+y, -0.5-z$; III $x, -1+y, z$; IV $x, 1+y, z$.

**Table 3** Infrared absorption bands in the 800–900 $cm^{-1}$ region of selected *cis*- and *trans*-[M(cyclam)$Cl_2$]X complexes

| Geometry | M | X | N–H vibration/$cm^{-1}$ | $CH_2$ vibration/$cm^{-1}$ | Ref. |
|---|---|---|---|---|---|
| *cis* | Cr | Cl | 872m 862m (sh) 854m | 815w 805m | 35 |
| *cis* | Mn | Cl | 923m 858s 844s | 807w (sh) 795m | * |
| *cis* | Fe | Cl | 866s 858m 850s | 808m 794s | 36 |
| *cis* | Co | Cl | 890w 872s 859s 841w | 824w 808s | 36 |
| *trans* | Cr | Cl | 890s 882s | 804s | 35 |
| *trans* | Mn | Cl | 880s | 795m | * |
| *trans* | Fe | $ClO_4$ | 890s 888s (sh) | 810m | 36 |
| *trans* | Co | Cl | 906s 888s | 818s | 36 |

* This work.



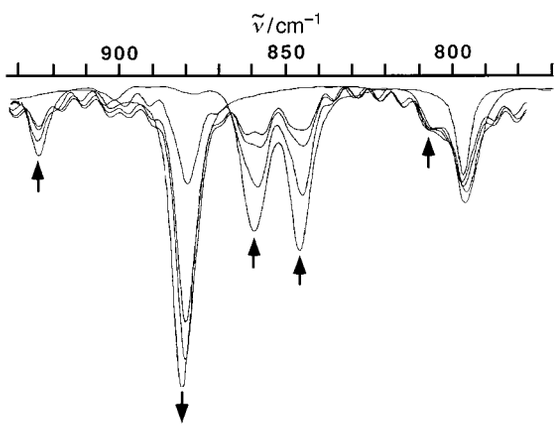


**Fig. 3** Evolution of IR spectra of *cis*- to *trans*-[Mn(cyclam)$Cl_2$]Cl

Fig. 3. This decrease in band number is consistent with the higher symmetry of the *trans* compared to the *cis* isomer.

## Electrochemistry

Evidence of the reductive isomerisation *trans*-$Mn^{III}\longrightarrow$ *cis*-$Mn^{II}$ has been observed by cyclic voltammetry experiments starting from the *trans*-[$Mn^{III}$(cyclam)$Cl_2$]Cl complex. As shown in Fig. 4(*a*), the first positive scan displays only a capacitive current (no electrochemically active species being present and thus no oxidation to $Mn^{IV}$ takes place up to 0.6 V *vs*. SCE). However, after the chemically irreversible reduction of the *trans*-manganese(III) isomer, a reversible oxidation wave appears at $E^{\circ}_{c} = 0.3$ V and a parallel decrease in cathodic current is noted during the second cycle of the voltammogram. This diminution in cathodic current is consistent with the formation of the *cis*-manganese(II) isomer produced and characterised by its reversible oxidation wave signature during the first cycle. However, the irreversible reduction of the *trans*-manganese(III) complex becomes electrochemically quasi-reversible at scan rates approaching 20 V $s^{-1}$. Exclusive formation of the *cis*-manganese(II) complex was observed during bulk reductive electrolysis of the *trans*-manganese(III) isomer. Furthermore, the cathodic stationary current for the reduction of the *trans*-[$Mn^{III}$(cyclam)$Cl_2$]Cl complex before the coulometry experiment and the resulting anodic stationary current

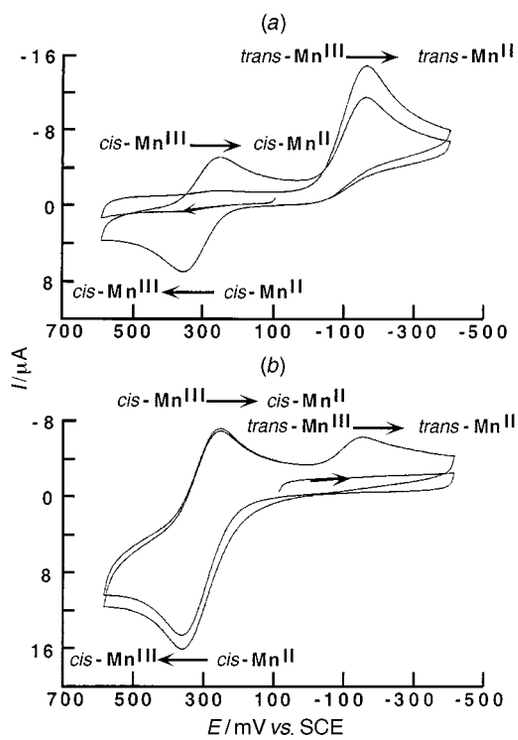


**Fig. 4** Cyclic voltammograms of (*a*) *trans*-[Mn(cyclam)$Cl_2$]Cl and (*b*) *cis*-[Mn(cyclam)$Cl_2$] in dmso containing 0.1 M $NBu^{n}_{4}PF_6$. [Complex] = 2 mM, scan rate = 100 mV $s^{-1}$, glassy carbon working electrode ($r$ = 1.5 mm)

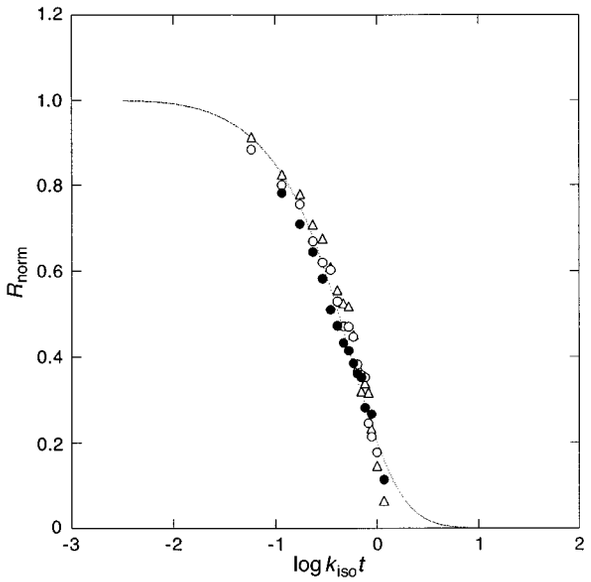


**Fig. 5** Variation in the normalised current ratios $R_{norm}$ with the parameter log $k_{iso}t$ for the electrochemical step–chemical step mechanism in double-step chronoamperometry. The initial potential was imposed at +0.1 V changed to −0.4 V for a time $t$ and returned to +0.1 V. Comparison to the theoretical curve for various concentrations of *trans*-[Mn(cyclam)$Cl_2$]Cl : 0.5 (△), 1.0 (○) and 2.0 mM (●)

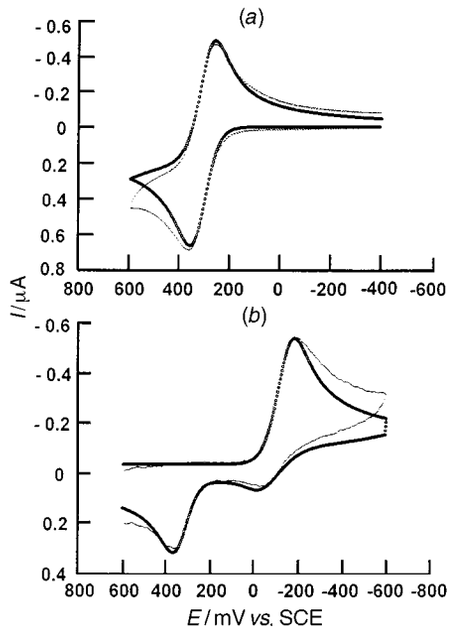


**Fig. 6** Experimental and simulated cyclic voltammograms for (*a*) a 2 mM solution of $MnCl_2 \cdot 4H_2O$ + cyclam at 500 mV $s^{-1}$ and (*b*) a 2 mM solution of *trans*-[Mn(cyclam)$Cl_2$]Cl at 1.28 V $s^{-1}$. Experimental data (—); Simulation (○) according to the set of parameters reported in Table 4 and $k_{iso} = 5.8\ s^{-1}$, $k_{-iso} = 0.1\ s^{-1}$ (see text)

for the *cis*-[$Mn^{II}$(cyclam)$Cl_2$] complex produced are equal in the RDE experiments, indicative of a quantitative conversion.

Since the chemical *trans*-$Mn^{III} \longrightarrow$ *cis*-$Mn^{II}$ reductive isomerisation was of particular interest, double-step chronoamperometry experiments were performed on solutions of the *trans*-[$Mn^{III}$(cyclam)$Cl_2$]Cl complex. The normalised current ratios were plotted as a function of log $k_{iso}t$ for a mechanism where one molecule of *trans*-manganese(II) species isomerises to the *cis* complex. A good agreement between the simulated normalised current ratio $R_{norm}$ for the electrochemical step–chemical step mechanism ($R_{norm}$ *vs.* log $k_{iso}t$) and the experimental data was obtained over a concentration range from 0.5 to 2.0 mM. Similarly, neither addition of free chloride ions {40 equivalents [$N(PPh_3)_2$]Cl nor deliberately added water (150 equivalents) affects the variation of $R_{norm}$. Therefore, the overall kinetics of the chemical isomerisation is not bimolecular and does not involve chloride ions or water molecules. The results of the chronoamperometric analysis are depicted on Fig. 5. The rate constant, $k_{iso}$, is equal to 5.8 ± 0.6 $s^{-1}$.

Cyclic voltammetry was also performed upon the *cis*-[$Mn^{II}$(cyclam)$Cl_2$] generated *in situ* by addition of cyclam to a solution of $MnCl_2 \cdot 4H_2O$ in dmso. The electrochemical oxidation potential ($E_{\frac{1}{2}}$) of this reduced *cis* complex is identical to the reduction potential of the *cis*-manganese(III) complex the preparation of which is described herein [Fig. 4(*b*)]. Upon oxidation of this *cis*-manganese(II) complex the resulting *cis*-manganese(III) complex undergoes a chemical isomerisation reaction to form a small quantity of the corresponding *trans* isomer during a voltammetric scan at scan rate of 100 mV $s^{-1}$. Simulation of the corresponding set of voltammograms allows one to evaluate the corresponding rate constant as *ca.* $k_{-iso} = 0.1\ s^{-1}$. However, the one-electron oxidation of *cis*-[$Mn^{II}$(cyclam)$Cl_2$] is electrochemically reversible and becomes chemically reversible when scan rates approach 1 V $s^{-1}$ in the cyclic voltammetry [Fig. 6(*a*)]. It must be emphasised that this *cis*-$Mn^{III} \longrightarrow$ *trans*–$Mn^{III}$ isomerisation between the oxidised states does not interfere at all with our above kinetic determinations (*i.e.* that relative to the *trans*-$Mn^{II} \longrightarrow$ *cis*–$Mn^{II}$ isomerisation occurring between the reduced states) because of the design of the experiments and because of the largely different half-lives of *trans*-$Mn^{II}$ ($k_{iso} = 5.8\ s^{-1}$) and *cis*-$Mn^{III}$ ($k_{-iso} = 0.1\ s^{-1}$).

**Table 4** Electrochemical data for *cis*- and *trans*-[$Mn^{III}$(cyclam)$Cl_2$]Cl obtained through simulation of their cyclic voltammograms

| Parameter | *cis*-[Mn(cyclam)-$Cl_2$]Cl | *trans*-[Mn(cyclam)-$Cl_2$]Cl |
|---|---|---|
| Standard potential $E°$/V *vs.* SCE | 0.305 | −0.090 |
| Heterogeneous rate constant, $k_s$/cm $s^{-1}$ | 0.004 | 0.002 |
| Diffusion coefficient, $D$/$cm^2$ $s^{-1}$ | $9.9 \times 10^{-7}$ | $1.1 \times 10^{-6}$ |
| Transfer coefficient α | 0.5 | 0.5 |

Simulation of the cyclic voltammograms was achieved using the DIGISIM program.[28] From the cyclic voltammetry data of *cis*-[$Mn^{II}$(cyclam)$Cl_2$] generated *in situ*, the $E°_c$ (*cis*-$Mn^{III} \longrightarrow$ *cis*-$Mn^{II}$) = 0.305 V was calculated over several scan rates (100, 500, and 700 mV $s^{-1}$). Other electrochemical parameters of interest such as the transfer coefficient (α), the heterogeneous rate constant ($k_s$), and the diffusion coefficient ($D$) were also optimised over these scan rates (see Table 4). The correspondence between the simulation and the experimental voltammograms is shown in Fig. 6(*a*). Taking into account these results for the *cis*-manganese(II) complex and the rate constant, $k_{iso}$, given by the chronoamperometry experiments, the voltammograms of *trans*-[$Mn^{III}$(cyclam)$Cl_2$]Cl were also simulated over a large range of scan rates (0.5, 1.3 and 5.1 V $s^{-1}$). The good agreement between the experimental data and simulations led to the determination of all electrochemical parameters (see Table 4), among which $E°_t$ (*trans*-$Mn^{III} \longrightarrow$ *trans*-$Mn^{II}$) = −0.090 V was calculated. Fig 6(*b*) illustrates the good agreement between simulated and experimental voltammograms.

This *trans*-$Mn^{II} \longrightarrow$ *cis*-$Mn^{II}$ isomerisation is of particular interest since previous studies performed with the iron analogue, *trans*-[$Fe^{III}$(cyclam)$Cl_2$]Cl, in dmso, do not reveal such a transformation.[42] Moreover, only the isomerisation *cis*-$Fe^{III} \longrightarrow$ *trans*-$Fe^{III}$ is noted in aqueous media; little transformation is observed in dmso solution even when heating up to 90 °C.[42] In aqueous media *cis*-[$Mn^{III}$(cyclam)$Cl_2$]Cl also isomerises to form the *trans* complex but the reverse reaction is not

observed. The equilibrium constant ratio $K_{iso}:K'_{iso}$ [where $K_{iso}$ is the equilibrium constant *cis*:*trans* at the manganese(II) level and $K'_{iso}$ that at the manganese(III) one] can be determined by considering the thermodynamic cycle in Scheme 1. It has to be noted that for the nickel cyclam derivative a similar cycle has been proposed upon oxidation of $Ni^{II}$ to $Ni^{III}$.[43] Based on the experimental values of $E°_t$ and $E°_c$ determined above, one obtains $K_{iso}:K'_{iso} \leqslant 5 \times 10^6$. Such a value explains why the *trans* to *cis* isomerisation is irreversible at the manganese(II) level while it is irreversible in the *cis* to *trans* direction at the manganese(III) stage. The different rate constants for $Mn^{II}$ and $Mn^{III}$ are typical, as manganese(II) complexes give much faster ligand exchange rates than manganese(III) species.[44]

$$\begin{array}{ccc} trans\text{-}Mn^{III}Cl_2 & \xrightarrow{-FE°_t} & trans\text{-}Mn^{II}Cl_2 \\ -RT\ln K'_{iso} \downarrow & & \downarrow -RT\ln K_{iso} \\ cis\text{-}Mn^{III}Cl_2 & \xleftarrow{+FE°_c} & cis\text{-}Mn^{II}Cl_2 \end{array}$$

**Scheme 1** $K_{iso}/K'_{iso} = \exp[(F/RT)(E°_c - E°_t)]$

Furthermore, no kinetically controlled predissociation of the chloride ligand from *trans*-[$Mn^{III}$(cyclam)$Cl_2$]Cl or *cis*-[$Mn^{II}$(cyclam)$Cl_2$] isomers occurs as determined by cyclic voltammetry using addition of different excesses of an internal chloride standard [$N(PPh_3)_2$]Cl. Despite this lack of any kinetic signature of a chloride ion dissociation/recombination, such a reaction may well occur whenever the dissociation is fast and reversible, equations (1) and (2). Indeed, considering a steady

$$trans\text{-}Mn^{II}Cl_2 \underset{k_{-1}}{\overset{k_1}{\rightleftharpoons}} Mn^{II}Cl^+ + Cl^- \quad (1)$$

$$Cl^- + Mn^{II}Cl^+ \underset{k_{-2}}{\overset{k_2}{\rightleftharpoons}} cis\text{-}Mn^{II}Cl_2 \quad (2)$$

state kinetic behaviour of the transient $Mn^{II}Cl^+$ intermediate, the overall kinetic behaviour of the sequence (1) + (2) is equivalent to that of a direct reversible reaction (3) with $k_{iso} = k_1k_2/$

$$trans\text{-}Mn^{II}Cl_2 \underset{k_{-iso}}{\overset{k_{iso}}{\rightleftharpoons}} cis\text{-}Mn^{II}Cl_2 \quad (3)$$

$(k_{-1} + k_2)$ and $k_{-iso} = k_{-1}k_{-2}/(k_{-1} + k_2)$. Thus, despite the real mechanism involving most likely dissociation and recombination of the $Cl^-$ ligand, this is not apparent kinetically and no effect of added chloride ions can be observed. The same situation obviously may occur for the reverse overall process when an authentic solution of *cis*-[$Mn^{II}$(cyclam)$Cl_2$] is oxidised [Fig. 4(*b*)].

## Conclusion

A novel synthesis of a new type of cyclam manganese complex, *cis*-dichlorocyclammanganese(III) chloride, has been described. The *cis* and *trans* isomers could be conveniently distinguished by IR spectroscopy. The *cis*-$Mn^{III} \longrightarrow$ *trans*-$Mn^{III}$ isomerisation reaction is enhanced by the presence of water as was previously reported for the corresponding iron and cobalt compounds[36] as deduced by IR spectroscopy. The two overall isomerisation reactions were also characterised by cyclic voltammetry experiments: *trans*-$Mn^{III} \longrightarrow$ *cis*-$Mn^{II}$ and *cis*-$Mn^{II} \longrightarrow$ *trans*-$Mn^{III}$. No kinetically limiting predissociation of the chloride ligand from *trans*-[$Mn^{III}$(cyclam)$Cl_2$]Cl or *cis*-[$Mn^{II}$(cyclam)$Cl_2$] isomers is associated with these electrochemical step–chemical step mechanisms occurs as determined in experiments with an internal chloride standard, [$N(PPh_3)_2$]Cl. The overall unimolecular *trans*-$Mn^{III} \longrightarrow$ *cis*-$Mn^{II}$ isomerisation reaction was characterised by double-step chronoamperometry and modelling of its cyclic voltammogram was made over a large timescale. The rate constant, $k_{iso}$, is equal to $5.8 \pm 0.6\ s^{-1}$.

No such electrochemically induced *trans*-$M^{III} \longrightarrow$ *cis*-$M^{II}$ in dmso has been noted for iron or cobalt complexes of the type *trans*-[$M^{III}$(cyclam)$Cl_2$]Cl. Thus, our current research efforts are focussed upon how the size of the metal and the macrocyclic cavity can affect this reaction ($k_{-iso} = 0.1\ s^{-1}$).

## Acknowledgements

Centre National de la Recherche Scientifique is gratefully acknowledged for financial support of this research in Dijon (UMR 5633 and 5632), Nancy (UPRESA 7036), and Paris (URA 1679). Financial support from Ecole Normale Superieure is also gratefully appreciated. G. B. acknowledges the Région-Bourgogne for a post-doctoral fellowship.

## References

1 Y. Kono and I. Fridovich, *J. Biol. Chem.*, 1983, **258**, 13 646.
2 M. L. Ludwig, K. A. Pattridge and W. C. Stallings, *Metabolism and Enzyme Function*, New York, 1986.
3 A. Willing, H. Follmann and G. Auling, *Eur. J. Biochem.*, 1988, **175**, 167.
4 J. H. Koek, S. W. Russell, L. Van der Wolf, R. Hage, J. B. Warnaar, A. L. Spek and L. DelPizzo, *J. Chem. Soc.*, *Dalton Trans.*, 1996, 353.
5 N. Kitajima, M. Osawa, S. Imai, K. Fujisawa, Y. Morooka, K. Heerwegh, C. A. Reed and P. D. W. Boyd, *Inorg. Chem.*, 1994, **33**, 4613.
6 Y. Naruta and M. Sasayama, *J. Chem. Soc.*, *Chem. Commun.*, 1994, 2667.
7 V. L. Pecoraro, M. J. Baldwin and A. Gelasco, *Chem. Rev.*, 1994, **94**, 807.
8 D. P. Riley and R. H. Weiss, *J. Am. Chem. Soc.*, 1994, **116**, 387.
9 D. E. De Vos, J. L. Meinershagen and T. Bein, *Angew. Chem.*, *Int. Ed. Engl.*, 1996, **35**, 2211.
10 D. E. De Vos and T. Bein, *J. Organomet. Chem.*, 1996, **520**, 195.
11 R. Hage, *Eur. Pat.* 0549 272 A1, 1993.
12 R. Hage, J. E. Iburg, J. Kerschner, J. H. Koek, E. L. M. Lempers, R. J. Martens, U. S. Racherla, S. W. Russell, T. Swarthoff, M. R. P. Vanvliet, J. B. Warnaar, L. Vanderwolf and B. Krijnen, *Nature* (*London*), 1994, **369**, 637.
13 S. M. Harriot-Jureller and J. L. Kerschner, *Eur. Pat.* 0544 519 A2, 1993.
14 R. J. Martens and S. Ton, *Eur. Pat.* 0544 490 A1, 1993.
15 V. C. Quee-Smith, L. Delpizzo, S. H. Jureller and J. L. Kerschner, *Inorg. Chem.*, 1996, **35**, 6461.
16 K. Wieghardt, U. Bossek, D. Ventur and J. Weiss, *J. Chem. Soc.*, *Chem. Commun.*, 1985, 347.
17 K. Wieghardt, U. Bossek, L. Zsolnai, G. Huttner, G. Blondin, J.-J. Girerd and F. Babonneau, *J. Chem. Soc.*, *Chem. Commun.*, 1987, 651.
18 K. J. Brewer, A. Liegeois, J. W. Otvos, M. Calvin and L. O. Spreer, *J. Chem. Soc.*, *Chem Commun.*, 1988, 1219.
19 K. J. Brewer, M. Calvin, R. S. Lumpkin, J. W. Otvos and L. O. Spreer, *Inorg. Chem.*, 1989, **28**, 4446.
20 P. A. Goodson and D. J. Hodgson, *Inorg. Chim. Acta*, 1990, **172**, 49.
21 P. A. Daugherty, J. Glerup, P. A. Goodson, D. J. Hodgson and K. Michelsen, *Acta Chem. Scand.*, 1991, **45**, 244.
22 W. Nam and J. S. Valentine, *J. Am. Chem. Soc.*, 1993, **115**, 1772.
23 Y. Park, S. Kim and H. Na, *J. Korean Chem. Soc.*, 1993, **37**, 648.
24 A. M. Bond, R. Colton and J. J. Jackowski, *Inorg. Chem.*, 1975, **14**, 274.
25 M. F. C. Guedes da Silva, J. J. R. Frausto da Silva, A. J. L. Pombeiro, C. Amatore and J. N. Verpeaux, *Organometallics*, 1994, **13**, 3943.
26 F. L. Wimmer, M. R. Snow and A. M. Bond, *Inorg. Chem.*, 1974, **13**, 1617.
27 R. A. Rader and D. R. McMillin, *Inorg. Chem.*, 1979, **18**, 545.
28 M. Rudolph, D. P. Reddy and S. W. Feldberg, *Anal. Chem.*, 1994, **66**, 589A.
29 E. K. Barefield, *Inorg. Chem.*, 1972, **11**, 2273.
30 E. K. Barefield, F. Wagner, A. W. Herlinger and A. R. Dahl, *Inorg. Synth.*, 1976, **16**, 220.
31 R. H. Blessing, *Crystallogr. Rev.*, 1987, **1**, 3.

32 G. M. Sheldrick, SHELX 76, Program for Crystal Structure Determinations, University of Göttingen, 1976.
33 C. K. Johnson, ORTEP, Report ORNL-3794, 2nd revision, Oak Ridge National Laboratory, TN, 1970.
34 C. K. Poon and M. L. Tobe, *J. Chem. Soc. A*, 1968, 1549.
35 C. K. Poon and K. C. Pun, *Inorg. Chem.*, 1980, **19**, 568.
36 P. K. Chan and C. K. Poon, *J. Chem. Soc.*, *Dalton Trans.*, 1976, 858.
37 M. E. Sosa-Torres and R. A. Toscano, *Acta Crystallogr.*, *Sect. C*, 1997, **53**, 1585.
38 N. W. Alcock, A. Berry and P. Moore, *Acta Crystallogr.*, *Sect. C*, 1992, **48**, 16.
39 A. Bakac and J. H. Espenson, *Inorg. Chem.*, 1987, **26**, 4353.
40 B. Bosnich, C. K. Poon and M. L. Tobe, *Inorg. Chem.*, 1965, **4**, 1102.
41 G. A. Jeffrey and J. Mitra, *Acta Crystallogr.*, *Sect. B,* 1983, **39**, 469.
42 R. Guilard, O. Siri, A. Tabard, G. Broeker, P. Richard, D. J. Nurco and K. M. Smith, *J. Chem. Soc.*, *Dalton Trans.*, 1997, 3459.
43 D. T. Pierce, T. L. Hatfield, E. J. Billo and Y. Ping, *Inorg. Chem.*, 1997, **36**, 2950.
44 V. L. Pecoraro, *Manganese Redox Enzymes*, VCH, New York, 1992.

*Received* 30*th January* 1998; *Paper* 8/00824H